Stable overexpression of Nup88 enhances HeLa cell migration through independent regulation of Kif7 and Gli1

MASAKI MAKISE, RYOTA UCHIMURA, AYANO SHIRAISHI and AKIHIKO KUNIYASU

Laboratory of Molecular Cell Pharmacology, Faculty of Pharmaceutical Sciences, Sojo University, Kumamoto 860-0082, Japan

Received November 21, 2025; Accepted July 6, 2026

DOI: 10.3892/or.2026.9170

Abstract. Elevated expression of nucleoporin (Nup) 88 is often observed in various types of cancer and correlates with tumor grade. However, the underlying molecular mechanism by which Nup88 induces cancer malignancy remains unclear. The present study showed that stable overexpression of Nup88 in HeLa cells enhanced cell migration by modulating the expression of kinesin family member (Kif) 7 and glioma-associated oncogene homolog (Gli) 1. The expression level of Kif7, a negative regulator of the Hedgehog (Hh) pathway acting through the processing of Gli2 and Gli3, was markedly reduced at both the mRNA and protein levels in Nup88 overexpressing HeLa cells. The reduced expression of Kif7 was restored by treatment with a DNA methylation inhibitor, suggesting epigenetic regulation. Co-overexpression of a truncated Kif7 (514-1343 aa), which possesses a large part of the Gli2 binding domain, suppressed the Nup88-induced migration, suggesting that the downregulation of Kif7 contributed to the enhanced cell migration. In parallel, Gli1 expression was elevated through activation of the MEK-ERK pathway and its knockdown markedly suppressed Nup88-induced cell migration. Although both Kif7 and Gli1 are components of the Hh pathway, neither the knockdown of Kif7 nor the overexpression of Gli1 affected the expression of the other. Instead, the truncated Kif7 (514-1343 aa) physically interacted with Gli1, suggesting that Kif7 suppressed enhanced migration by inhibiting Gli1 function. These findings revealed that Nup88 promotes cell migration by modulating the expression of Kif7 and Gli1, providing new insight into the mechanism of Nup88-driven malignancy.

Correspondence to: Dr Masaki Makise, Laboratory of Molecular Cell Pharmacology, Faculty of Pharmaceutical Sciences, Sojo University, 4-22-1 Ikeda, Nishi-ku, Kumamoto 860-0082, Japan
E-mail: makise@ph.sojo-u.ac.jp

Abbreviations: FG, phenylalanine and glycine; Gli, glioma-associated oncogene homolog; Hh, Hedgehog; KIF, kinesin family member; NPCs, nuclear pore complexes; Nups, nucleoporins

Key words: nucleoporin 88, cancer, migration, hedgehog signaling, kinesin family member 7, glioma-associated oncogene homolog 1, ERK

Introduction

Bidirectional trafficking of biological macromolecules between the nucleus and the cytoplasm in eukaryotic cells is mediated by the nuclear pore complexes (NPCs). The NPCs span the inner and outer nuclear membranes and act as gatekeepers by regulating molecular transit. Each mammalian NPC is made up of a large cylindrical hollow structure composed of multiple copies of more than 30 distinct polypeptides, termed nucleoporins (Nups) (1). Selective nuclear transport via NPCs is regulated primarily by the meshwork formed in the central pore of NPCs. About one-third of Nups contain phenylalanine and glycine (FG) repeats, which comprise the inner central pore of NPCs. The FG repeats serve as diffusion barriers for limiting the passage of macromolecules as well as docking sites for nuclear transport receptors that mediate cargo transport through NPCs (2-4). In addition to their role in nuclear transport, Nups are implicated in various cellular processes, such as mitosis, gene regulation, DNA repair and development (5,6). As such, dysregulation of Nups is associated with various human disorders, including cancer (7).

Nucleoporin (Nup) 88 is a non-FG Nup located primarily on the cytoplasmic side of NPCs where Nup88 interacts with other Nups and participates in nuclear export (8-12). Notably, high levels of Nup88 expression in the cytoplasm have been reported in a variety of tumor tissues, such as endometrial cancer, colorectal cancer, breast cancer, cervical cancer and hepatocellular carcinoma (13-20). As this aberrant expression was associated with the tumor grade, Nup88 appears to be involved in cancer malignancy (21). We previously reported that Nup88 promotes cell migration by inducing matrix metalloproteinase-12 (22). However, its effect was relatively modest, implying that other factors additionally contribute to Nup88-dependent migration.

Elevated expression of glioma-associated oncogene homolog (Gli) 1 is also associated with several malignant phenotypes of cancer, including anti-apoptotic effects, metastasis, angiogenesis, cancer drug resistance and maintenance of cancer stem cells (23). In mammalian cells, expression of Gli1 is regulated at the transcriptional level by the Hedgehog (Hh) pathway and oncogenic signaling (23,24). The Hh pathway regulates expression of Gli1 directly via the effector transcription factors Gli2 and Gli3. Although Gli2 and Gli3 function in a context-dependent manner, Gli2 and Gli3 generally act as a transcriptional activator and a transcriptional repressor, respectively (25).

The activity of Gli2/3 is regulated primarily by kinesin family member (Kif) 7, which controls their processing and nuclear translocation in the Hh pathway (26,27). In the absence of Hh ligands, Kif7-free Gli2/3 are processed into transcriptional repressors, whereas Gli2/3 bound to Kif7 are protected from processing, but their activation is inhibited. Upon Hh pathway activation, Kif7 releases Gli2/3, allowing their activation and nuclear translocation as transcriptional activators (28). While Kif7 acts as a negative regulator of Gli2/3, it can function as a tissue-specific positive regulator during mouse embryonic development (27). The downregulation of Kif7 is linked to malignant phenotypes in cancer cells. While the epigenetic suppression of Kif7 has been reported in some prostate cancer cell lines (29), the molecular mechanism that triggers this decrease in expression has not been elucidated. In addition to the Hh pathway, the expression of Gli1 is often driven by oncogenic signaling, such as Rat sarcoma-rapidly accelerated fibrosarcoma-mitogen-activated protein kinase/ERK kinase-extracellular signal-regulated kinase (Raf-Ras-MEK-ERK) signaling, in cancer cells. However, the regulation of Gli1 expression by oncogenic signaling is complex and poorly understood.

The present study focused on cervical cancer, which remains one of the leading causes of cancer-related mortality in women worldwide, largely due to its high potential for metastasis and recurrence (30,31). Cervical cancer is known to be caused by persistent infection with high-risk human papillomaviruses, whose oncoproteins (E6 and E7) facilitate malignant transformation by degrading tumor suppressors p53 and pRb (31). Given this clinical significance, we have consistently utilized the HeLa cervical cancer cell line as a robust model of aggressive malignancy to investigate the molecular mechanisms of Nup88-driven progression. The present study found that stable overexpression of Nup88 in HeLa cells induced not only the downregulation of Kif7 but also the upregulation of Gli1. Furthermore, it was found that changes in their expression markedly impact the HeLa cell motility. Based on these findings, the present study proposed a mechanistic model in which Nup88 promotes cell migration through the independent modulation of Kif7 and Gli1 expression, providing new insight into Nup88-driven malignancy.

Materials and methods

Cell lines and cell culture. Stable cell lines that inducibly overexpress GFP and GFP-tagged Nup88 in response to doxycycline were previously established from HeLa R19 cells containing a single Flp recombination site in the genome (32,33). Cells were cultured in Dulbecco's modified Eagle's medium (DMEM; FUJIFILM Wako Pure Chemical Corporation) supplemented with 10% fetal bovine serum (HyClone™; Cytiva), penicillin/streptomycin (FUJIFILM Wako Pure Chemical Corporation) and 1 μg/ml doxycycline (Nacalai Tesque, Inc.) in a humidified atmosphere with 5% CO_2 at 37˚C.

Plasmids and small interfering (si)RNAs. pEGFP-N2-*NUP88*, a plasmid that overexpresses GFP-fused Nup88, was constructed previously (32). pEGFP-N2-*GLI1*, a plasmid that overexpresses GFP-tagged Gli1 was constructed as follows. The *GLI1* gene was obtained from pOTB7 coding *GLI1* cDNA by PCR using the following pair of oligonucleotide primers (Forward: 5'-CTCAAGCTTCGAATTCCGCCACCATGTTCAACTCGATGACCCCA-3', Reverse: 5'-GTCGACTGCAGAATTCGGCACTAGAGTTGAGGAATTCTGT-3'). The underlined sequences represent the regions complementary to the *GLI1* gene. The amplified product was cloned into the *Eco*RI site of pEGFP-N2 (Takara Bio, Inc.) using an In-Fusion HD Cloning Kit (Takara Bio, Inc.). The plasmids were transformed into competent cells via heat shock at 42˚C for 30 sec. After the addition of LB medium, the cells were incubated at 37˚C for 30 min and then cultured overnight on LB agar plate containing appropriate antibiotics. A plasmid that overexpresses Flag-tagged *GLI1* was constructed by replacing the eGFP gene in pEGFP-N2-*GLI1* with the 3xFLAG gene. pDPNR223 containing the truncated *KIF7* gene (ID100072702A), which encodes amino acid residues 514-1343 of full-length Kif7 (1343 aa), was purchased from DNAFORM. mCherry-tagged truncated *KIF7* [pmCherry-KIF7(514-1343)] was constructed as follows. The entire truncated *KIF7* in pDPNR223 was amplified by PCR using the following primer set (Forward: 5'-gtcgacggtaccgcgggcccgggcgccaccatggagcagtacaaactgca-3', Reverse: 5'-tccttgtagtcttggatcccgggcaggggttttttccggac-3') and cloned into pEGFP-N2 using an In-Fusion HD Cloning Kit. The underlined sequences represent the regions complementary to the *KIF7* gene. The eGFP gene in the plasmid was then swapped with the mCherry gene. siRNAs for control (cat. no. 4390843), *KIF7* (cat. no. 4427037, ID: s51568), *GLI1* (cat. no. 4427037, ID: s5816), *GLI2* (cat. no. 4427037, ID: s5817), *GLI3* (cat. no. 4427037, ID: s533814), and *KRAS* (cat. no. 4427038, ID: s7939) were purchased from Thermo Fisher Scientific, Inc.

Transfection of plasmids and siRNAs. Plasmids and siRNAs were transfected using Lipofectamine® LTX and Lipofectamine® RNAiMax reagent, respectively, according to the manufacturer's instructions (Invitrogen; Thermo Fisher Scientific, Inc.). The transfection complexes prepared were added to cells at room temperature, and the cells were then incubated at 37˚C in a CO_2 incubator. Subsequent experiments were performed 24 h after transfection for plasmids. For the siRNAs, cells were analyzed 48 h after transfection for *KRAS*, *GLI1*, *GLI2*, and *GLI3*-targeting siRNAs and 24 h after transfection for *KIF7*-targeting siRNA.

Reverse transcription-quantitative (RT-q) PCR. Total RNA was prepared from ~1x10^7 cells using an RNeasy Kit (Qiagen GmbH). RT-qPCR was performed using One Step TB® Green PrimeScript RT-PCR Kit II (Takara Bio, Inc.) and StepOnePlus™ (Applied Biosystems; Thermo Fisher Scientific, Inc.). All experiments using these kits and apparatus were performed according to the manufacturer's instructions or protocols. RT-qPCR conditions were as follows: Initial denaturation at 95˚C for 30 sec, followed by 40 cycles of 95˚C for 5 sec and 60˚C for 30 sec. The expression of genes of interest was assessed using the $2^{-\Delta\Delta Cq}$ method with human 18S rRNA (*RN18S1*) as the internal control for normalization (34). Oligonucleotide primers employed in this assay were as follows: RN18S1 Forward: 5'-CGGCTACCACATCCAAGGAA-3'; RN18S1 Reverse: 5'-GCTGGAATTACCGCGGCT-3';

KIF7 Forward: 5'-AGACGGAAGAGATCGCGGCATT-3'; KIF7 Reverse: 5'-CTGCTGTAGCACCTTCTCCATC-3'.

Antibodies and reagents. Antibodies used for immunoblotting were as follows: Anti-GFP (cat. no. 598), anti-RFP (cat.no.PM005),anti-α-tubulin(cat.no.PM054),andanti-β-actin (cat. no. PM053-7) from Medical & Biological Laboratories Co., Ltd.; anti-Kif7 (cat. no. ABS1458) and anti-FLAG® M2 (cat. no. F1804) from MilliporeSigma; anti-DNMT1 (D63A4; cat. no. 5032), anti-Gli1 (C68H3; cat. no. 3538), anti-p44/42 MAPK (ERK1/2; 137F5; cat. no. 4695), anti-phospho-p44/42 MAPK (Thr202/Tyr204; D13.14.4E; cat.no.4370P),anti-mTOR (cat. no. 2983), anti-p-mTOR (S2448) (cat. no. 2971), anti-AKT (cat. no. 9272), anti-phospho-AKT (Thr308) (cat. no. 9275), anti-phospho-AKT (Ser473) (cat. no. 4060P), anti-Smad2/3 (cat. no. 8685T), and anti-Lamin A/C (cat. no. 4777S) from Cell Signaling Technology, Inc.; anti-Nup88 (cat. no. 611896; BD Biosciences); anti-Gli2 (cat. no. 18989-1-AP), anti-phospho-ERK(1/2; Thr202/Tyr204; cat. no. 80031-1-RR), and anti-KRAS (cat. no. 12063-1-AP) from Proteintech Group, Inc.; anti-human/mouse Gli3 (cat. no. AF3690; R&D Systems); anti-phospho-mTOR (Ser2481) (cat. no. 09-343SP) from Merck Millipore. Peroxidase-conjugated goat anti-rabbit IgG (cat. no. 115-035-003) and anti-mouse IgG (cat. no. 115-035-062) were purchased from Jackson Immuno Research Laboratory, Inc. 5-Aza-2'-deoxycytidine (cat. no. A2232) and U0126 (cat. no. S1102) were purchased from Tokyo Chemical Industry and Selleck Biotechnology, respectively.

Fluorescence microscopy. Cells were seeded into 24-well plates containing coverslips ($3x10^4$ cells/well). After 2 days of culture, cells were washed once with PBS and fixed with 4% paraformaldehyde at 4˚C for 10 min. For indirect immunofluorescence imaging, the cells were permeabilized with 0.5% Triton X-100 in PBS for 10 min and then incubated with blocking buffer [3% bovine serum albumin (FUJIFILM Wako Pure Chemical Corporation), 0.05% Triton X-100 in PBS] for 1 h, followed by incubation with primary antibodies diluted 1:1,000 in the same blocking buffer for 1 h at room temperature. Following primary antibody incubation, the cells on coverslips were incubated with wash buffer (1.5% bovine serum albumin, 0.05% Triton X-100 in PBS) three times at 5 min intervals. Secondary antibodies conjugated with Alexa Fluor 568 or 488 (Thermo Fisher Scientific, Inc.) were diluted 1:1,000 in the same blocking buffer and then added for 1 h at room temperature in dark conditions. Following secondary antibody incubation, the cells on coverslips were washed three times in the same wash buffer. For direct fluorescence imaging, or after secondary antibody incubation in indirect immunofluorescence, cells were stained with Hoechst 33342 in PBS for 10 min at room temperature. Coverslips were mounted using ProLong Gold antifade reagent (Thermo Fisher Scientific, Inc.), and fluorescence was detected using a 20x objective of a FSX100 inverted fluorescence microscope (Olympus Corporation).

Immunoblotting. Whole cell lysates prepared with radioimmunoprecipitation assay (RIPA) buffer (FUJIFILM Wako Pure Chemical Corporation) were quantified using the Bradford assay reagent (Nacalai Tesque, Inc.) and then the lysates (~30 μg of protein per lane) were subjected to sodium dodecyl sulfate-polyacrylamide gel electrophoresis (SDS-PAGE) using 7, 10, or 12% gels depending on the molecular weight of the target proteins. Proteins separated in the gel were electroblotted onto an Immobilon-P transfer membrane (MilliporeSigma). The membrane was blocked with blocking buffer (5% skimmed milk and 0.05% Tween 20 in PBS) for 30 min at room temperature, followed by incubation overnight with primary antibody diluted 1:1,000 in dilution buffer (1% skimmed milk and 0.05% Tween 20 in PBS). The membrane was then washed three times with wash buffer (0.05% Tween 20 in PBS) for 5 min each and further incubated with peroxidase-conjugated secondary antibodies at 4˚C for 1 h. For each immunoblot, loading controls were detected on the same membrane as the corresponding target proteins. Chemiluminescence on the membrane produced by secondary antibodies in the presence of Luminate Crescendo Western HRP substrate (MilliporeSigma) was detected using a LAS2000 imaging analyzer (FUJIFILM Corporation). Densitometric analysis of target protein band intensities was performed using ImageJ version 1.54p (National Institutes of Health).

Live-cell single-cell imaging. Conditions used for live-cell single-cell imaging were established previously (22). Briefly, cells were seeded with $0.7x10^4$ cells on 4-well collagen-coated glass-bottom dishes (Matsunami Glass Ind., Ltd.) and incubated at 37˚C overnight with a phenol red-free culture medium in a humidified atmosphere with 5% CO_2. The medium was then changed just before setting the dishes on a stage top CO_2 incubator of a confocal microscope. Fluorescence signals from cells were acquired using a C2 confocal microscope system (Nikon, Tokyo, Japan) at 10 min intervals for 24 h. The migration velocity of each cell was analyzed using ImageJ version 1.54p (National Institutes of Health).

Chromatin immunoprecipitation (ChIP) assay. ChIP assays were performed using a SimpleChIP® Enzymatic Chromatin IP Kit (Cell Signaling Technology, Inc.), according to the manufacturer's instructions. Cells ($4x10^6$ cells per reaction) were cross-linked, lysed, and digested with Micrococcal Nuclease. Chromatin lysate (20 μg) was incubated with primary antibody (2 μg) overnight at 4˚C with rotation and 2% of the lysate was used as the Input control. Immune complexes captured with protein G magnetic beads were washed with low-salt and high-salt reagents. After cross-link reversal, purified DNA was subjected to PCR using Taq DNA polymerase (Takara Bio Inc.) under the following conditions: 95˚C for 5 min; 30 cycles of 95˚C for 30 sec, 55˚C for 30 sec, 72˚C for 30 sec and 72˚C for 1 min. PCR products were electrophoresed on a 2% agarose gel, visualized with ethidium bromide, and evaluated solely by visual inspection.

GFP pulldown assay. GFP-tagged proteins were retrieved from mammalian cell lysates using GFP-Trap A beads (Proteintech Group, Inc.). Cell lysates (500 μg; 1 mg/ml) containing GFP or GFP-tagged Gli1 and FLAG-tagged truncated Kif7 were incubated with the beads at 4˚C overnight. Beads were then washed three times with lysis buffer at 4˚C for 5 min and incubated with SDS sample buffer at 100˚C for 1 min to elute the bound proteins.

Data utilization from previous DNA microarray analysis. The expression data for *KIF7* used in this study were obtained from the DNA microarray analysis performed in our previous study (22). The raw dataset is accessible via GSE310626. *KIF7* expression data were extracted from this pre-existing dataset.

Statistical analysis. Statistical significance was evaluated using the paired t-test for most of the immunoblotting data. For the analysis of Fig. 3H, one-way analysis of variance followed by Dunnett's test was applied. Migration assays were analyzed using one-way ANOVA followed by the Tukey-Kramer multiple-comparison test. $P<0.05$ was considered to indicate a statistically significant difference.

Results

Decreased expression of Kif7 enhances the migration of HeLa cells overexpressing Nup88. We previously demonstrated by DNA microarray analysis that overexpression of Nup88 alters gene expression, which may influence cell motility (22). The present study, to identify additional factors involved in this Nup88-dependent migration, focused on *KIF7*, which showed a marked decrease in expression in our previous microarray analysis (22) (Table SI). Kif7 is a negative regulator of the Hh pathway that contributes to cancer development. It has been reported that in prostate cancer cell lines, the expression of *KIF7* is epigenetically repressed through hypermethylation of CpGs within its promoter (5' upstream) region, which promotes formation of the malignant phenotype (29). The present study therefore hypothesized that the downregulation of Kif7 could also contribute to motility in HeLa cells. To verify the DNA microarray results, previously established HeLa cell lines that stably overexpress GFP or GFP-tagged Nup88 were utilized (32). As shown in Fig. 1A and C, both proteins were overexpressed and exhibited the expected subcellular localization described previously (32). Specifically, immunoblotting with both anti-GFP and anti-Nup88 antibodies (Fig. 1C) allowed the present study to identify the Nup88-GFP fusion protein and verify its expression level relative to endogenous Nup88. Using these cell lines, the present study performed RT-PCR. This analysis confirmed that Kif7 expression at the RNA level was markedly decreased in the Nup88-overexpressing cells (Fig. 1B). This decreased expression of Kif7 was subsequently confirmed at the protein level (Fig. 1C). If the expression of Kif7 is epigenetically regulated, demethylation of DNA should restore its expression. Thus, it was examined whether the decreased expression of Kif7 was due to epigenetic regulation. Expression of Kif7 in cells stably overexpressing Nup88-GFP was monitored after treatment with a DNA methylation inhibitor, 5-aza-2'-deoxycytidine, which not only inhibits the activity of DNA methyltransferases (DNMTs) but also induces selective degradation of DNMT1 (35). In the experiment, cells overexpressing GFP or Nup88-GFP were cultured in standard medium containing the inhibitor (0 days) and then cells were collected every 2 days for up to 6 days to estimate the expression of Kif7 by immunoblotting. As shown in Fig. 1D, the expression of DNMT1 in both cell lines was markedly reduced 2 days after treatment with the inhibitor and the effect persisted for at least 6 days, indicating that the inhibitor remained effective throughout this time period. Under the given experimental conditions, expression of Kif7 in control cells was largely unaffected (Fig. 1D; lanes 1-4), while its expression in the Nup88-GFP overexpressing cells markedly recovered by days 4 and 6 (Fig. 1D; lanes 7 and 8). These results suggested that the expression of *KIF7* is regulated by DNA methylation in Nup88-overexpressing HeLa cells. It has been reported that *Drosophila* Nup88 binds to silent chromatin (36). Therefore, it was examined whether Nup88 binds to the *KIF7* promoter and contributes to DNA methylation. However, ChIP assays revealed that Nup88 did not specifically bind to the *KIF7* promoter (Fig. 1E).

Decreased expression of Kif7 has been reported to induce malignant phenotypes in prostate cancer cell lines, which can be suppressed by the overexpression of a Kif7 fragment (Kif7-CC) comprising a discontinuous coiled-coil and a globular C-terminal tail domain (29). Thus, complementation assays were performed to investigate whether the decreased expression of Kif7 also contributes to the malignant phenotype in Nup88-overexpressing cells. In these experiments, the migration activity of GFP- or Nup88-GFP-overexpressing cells was assessed using co-overexpression of mCherry or mCherry-tagged truncated Kif7 (514-1343 aa). The tagged protein was derived from human *KIF7* cDNA (BC112271) encoding a region largely comparable to Kif7-CC but lacking a portion of the Gli2-binding domain (481-541 aa). As shown in Fig. 2A and B, the expression of mCherry and mCherry-tagged truncated Kif7 was confirmed. Immunoblotting using anti-mCherry and anti-Kif7 antibodies confirmed that the transiently expressed proteins were correctly produced as intended fusion proteins at the expected molecular weights. Using these validated cells, live cell imaging analysis was performed, and it was found that, in cells expressing mCherry alone, the migration velocity of Nup88-GFP-overexpressing cells was almost twice that of GFP-overexpressing cells (Fig. 2C and Video S1). By contrast, in cells expressing mCherry-tagged truncated Kif7, the migration velocity of Nup88-GFP-overexpressing cells was suppressed to a level comparable to that of GFP-overexpressing cells (Fig. 2C and Video S1). These results indicate that downregulation of Kif7 contributes to the enhanced cell migration.

Expression of Gli1 is upregulated via the MEK-ERK pathway but not the Hh pathway in Nup88-overexpressing cells. Kif7 is a major negative regulator of the mammalian Hh pathway. Therefore, decreased expression of Kif7 was expected to activate the Hh pathway. Activation of the Hh pathway leads to increased expression of Gli1, which can promote malignant phenotypes in certain cancers (23). Thus, it was hypothesized that decreased expression of Kif7 might lead to malignant phenotypes by promoting expression of Gli1 via the Hh pathway in Nup88-overexpressing cells. To examine this possibility, immunoblotting was used to compare the expression of Gli1 between GFP- and Nup88-GFP-overexpressing cells. As expected, the expression of Gli1 was enhanced in Nup88-GFP-overexpressing cells (Fig. 3A and B). However, Gli1 expression was unaffected when both Gli2 and Gli3, which are involved in Gli1 transcription in the Hh pathway, were depleted by RNA interference in either GFP- or Nup88-GFP-overexpressing HeLa cells (Fig. 3C-H). These findings suggest that the Nup88-induced increase in Gli1

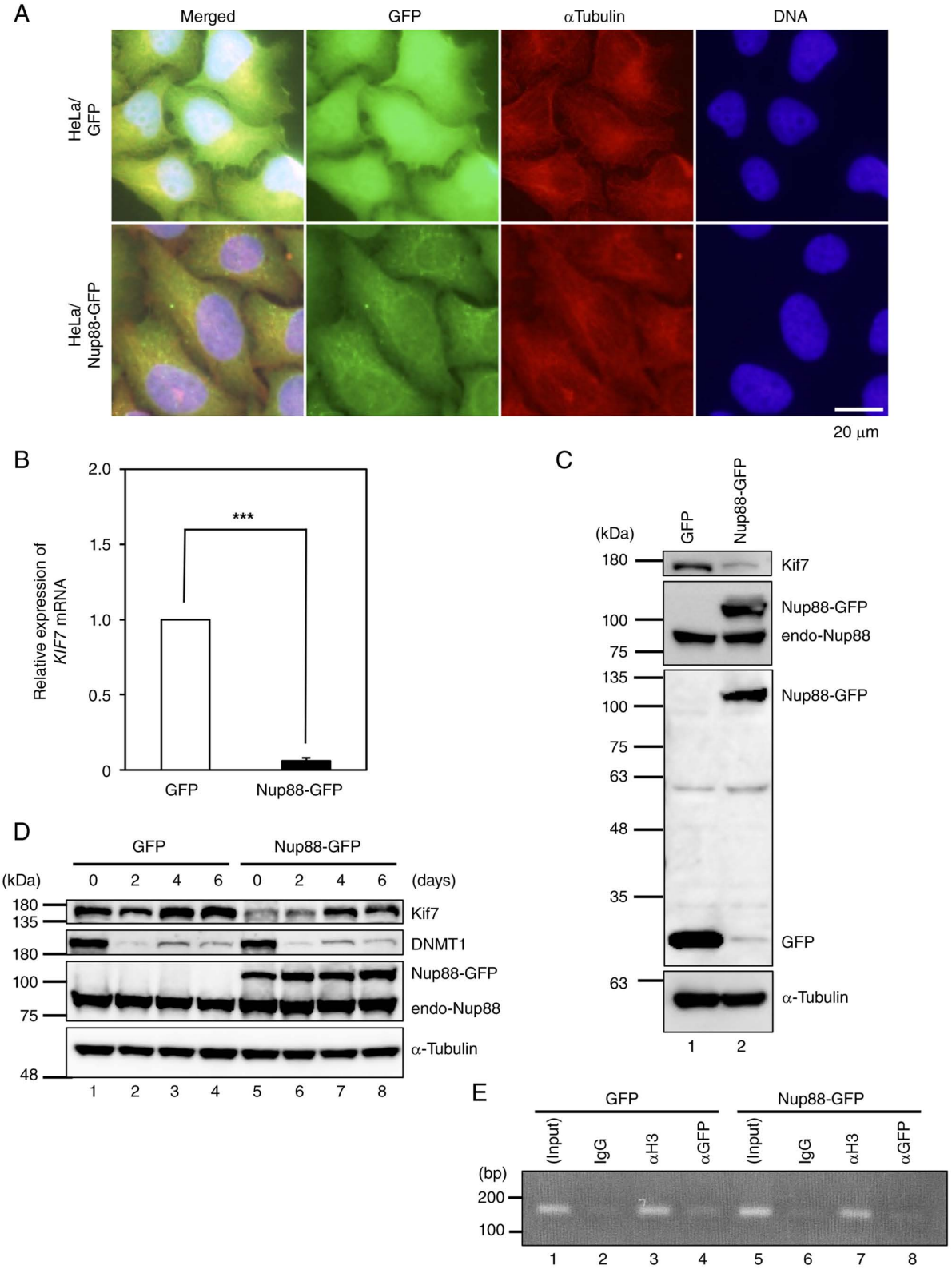

Figure 1. Decreased expression of Kif7 in Nup88-overexpressing HeLa cells. (A) Indirect immunofluorescence imaging of HeLa cells stably overexpressing GFP or GFP-tagged Nup88 (Nup88-GFP). (B) RT-qPCR for the gene expression of Kif7 in cells overexpressing GFP or Nup88-GFP. Data represent mean ± SD (n=3), ***P<0.001. (C) Immunoblotting for protein expression of Kif7 in cells overexpressing GFP or Nup88-GFP. Endogenous Nup88 is labeled as endo-Nup88. α-Tubulin was used as a loading control. Expression of Nup88-GFP was confirmed by immunoblotting using both anti-GFP and anti-Nup88 antibodies to verify the expression of the fusion protein. (D) Expression of Kif7 in cells incubated in the presence of a DNMT1 inhibitor. Cells overexpressing GFP (lanes 1-4) or Nup88-GFP (lanes 5-8) were incubated in complete medium containing 1 μM 5-aza-2'-deoxycytidine for 6 days. Cells were collected every 2 days, and their lysates were analyzed by immunoblotting. α-Tubulin was used as a loading control. (E) ChIP assay for Nup88 binding to the *KIF7* promoter region. After crosslinking, chromatin fractions were prepared from cells overexpressing GFP or Nup88-GFP. DNA fragments crosslinked to the protein of interest were immunoprecipitated using non-immune IgG (IgG; negative control), anti-histone H3 (αH3; positive control), or anti-GFP (αGFP). Crosslinking was then reversed, and the liberated DNA fragments were amplified by PCR using *KIF7* promoter-specific primers (see Materials and methods). Kif7, kinesin family member 7; Nup88, nucleoporin 88; RT-qPCR, reverse transcription-quantitative PCR; DNMT, DNA methyltransferases; ChIP, chromatin immunoprecipitation.

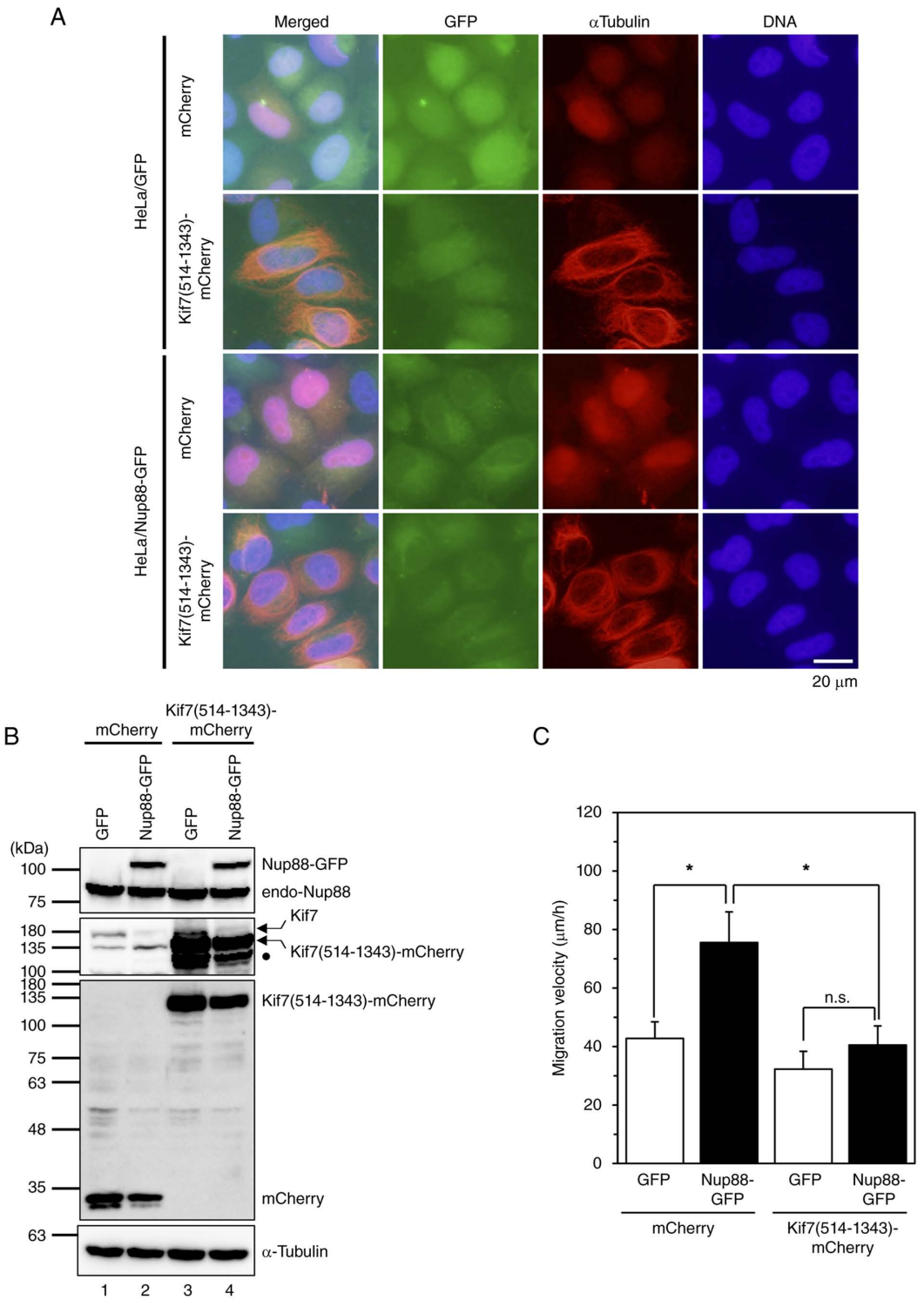

Figure 2. Enhanced migration of Nup88-overexpressing cells is suppressed by the co-overexpression of truncated Kif7. Co-overexpression of mCherry or Kif7(514-1343)-mCherry in cells overexpressing GFP or Nup88-GFP was confirmed by (A) direct fluorescence imaging and (B) immunoblotting. α-Tubulin was used as a loading control. Expression of Kif7(514-1343)-mCherry was confirmed by immunoblotting using both anti-RFP and anti-Kif7 antibodies to verify the expression of the fusion protein. Kif7(514-1343)-mCherry (lanes 3 and 4) was detected as an intensified signal at the same position as a nonspecific band observed in lanes 1 and 2. (C) Migration activity of the cells shown in (A) and (B). The average migration velocity was calculated by tracking the cells for 24 h. In GFP-overexpressing cells, the average migration velocities of cells expressing mCherry or Kif7(514-1343)-mCherry were 42.7 μm/h (n=62) and 32.3 μm/h (n=56), respectively. In Nup88-GFP-overexpressing cells, the average migration velocities of cells expressing mCherry or truncated Kif7-mCherry were 75.5 μm/h (n=63) and 40.5 μm/h (n=60), respectively. *P<0.05, n.s., not significant. The data in (C) are based on the values obtained from Data SI. Nup88, nucleoporin 88; Kif7, kinesin family member 7.

expression is independent of the Hh pathway. The expression of Gli1 is known to be regulated by oncogenic signaling pathways, such as phosphoinositide 3-kinase-Protein kinase B-mechanistic target of rapamycin (PI3K-AKT-mTOR), Transforming Growth Factor-β (TGF-β), and Ras-Rapidly accelerated Fibrosarcoma (Raf)-Mitogen-Activated Protein

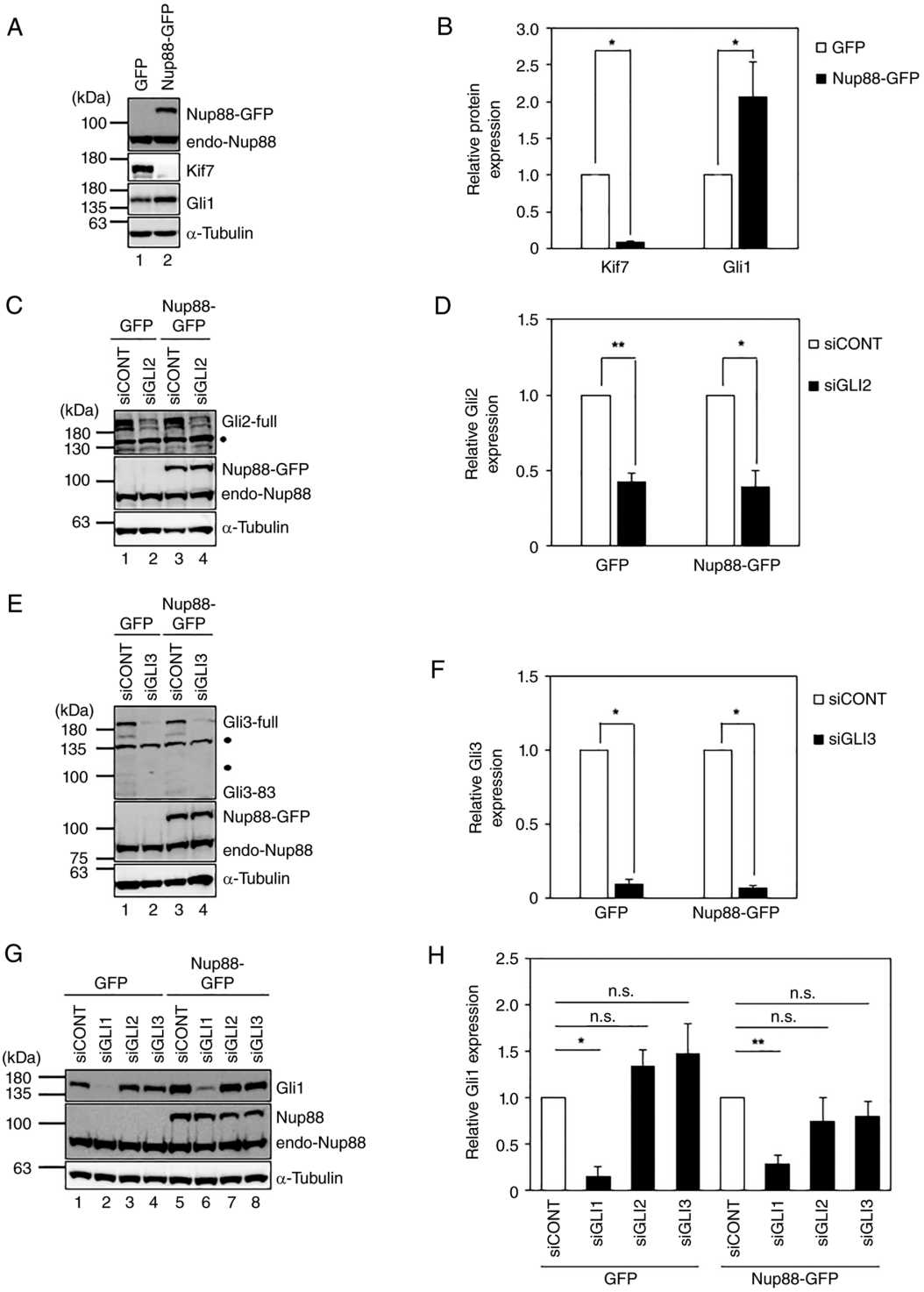

Figure 3. Increased expression of Gli1 in Nup88-overexpressing cells appears to be independent of the Hedgehog pathway. (A) Expression of Gli1 in cells overexpressing GFP or Nup88-GFP. (B) Statistical analysis of the expression of Kif7 and Gli1 shown in (A). Data represent mean ± SD (n=3). (C) Knockdown of Gli2. *GLI2*-specific siRNA was transfected into cells overexpressing GFP or Nup88-GFP, and Gli2 levels were analyzed by immunoblotting. (D) Statistical analysis of the expression of Gli2 shown in (C). Data represent mean ± SD (n=3). (E) Knockdown of Gli3. *GLI3*-specific siRNA was transfected into cells overexpressing GFP or Nup88-GFP, and the level of Gli3 was analyzed by immunoblotting. The very faint band at an apparent molecular mass of 83 kDa corresponds to the proteolytically processed form of full-length Gli3 (Gli3-83) (27). (F) Statistical analysis of the expression of Gli3 shown in (E). Data represent mean ± SD (n=3). (G) Effect of *GLI2* and *GLI3* knockdown on the expression of Gli1. The expression of Gli1 in both GFP- and Nup88-overexpressing cells with *GLI2* or *GLI3* knockdown, as shown in (C) and (E), was analyzed by immunoblotting. (H) Statistical analysis of the expression of Gli1 shown in (G). Data represent mean ± SD (n=3). α-Tubulin was used as a loading control. Closed circles in (C) and (E) indicate non-specific bands detected by the anti-Gli2 or anti-Gli3 antibodies, respectively. *P<0.05, **P<0.01, n.s., not significant. Gli1, glioma-associated oncogene homolog 1; Nup88, nucleoporin 88.

Kinase/ERK Kinase (MEK-ERK) (Ras-Raf-MEK-ERK) pathways (23,24). The present study therefore examined the involvement of these pathways in the expression of Gli1. Although PI3K-AKT-mTOR and TGF-β signaling were not specifically activated by the overexpression of Nup88 in HeLa cells (Fig. S1), the levels of phosphorylated (p) ERK1/2

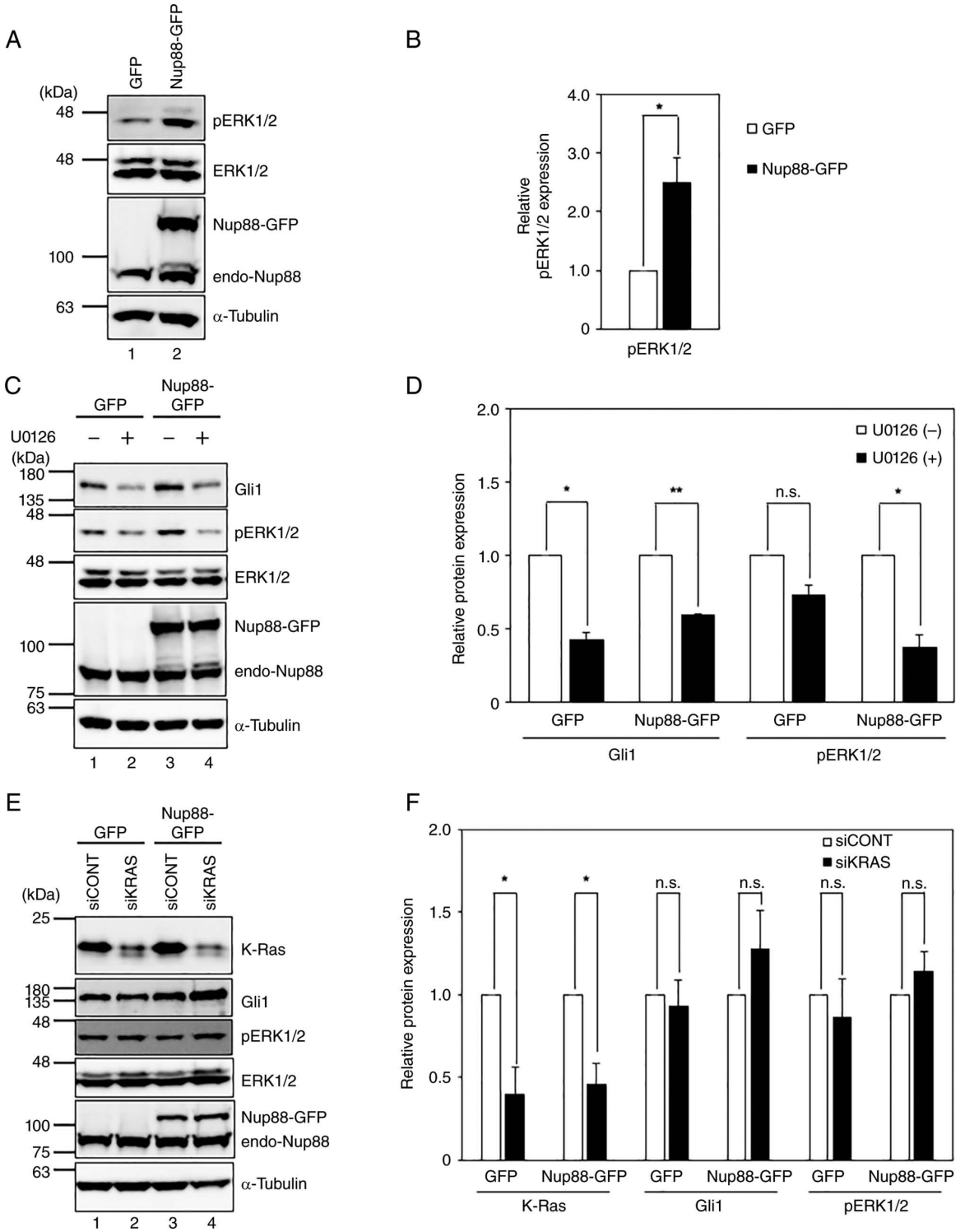

Figure 4. Increased expression of Gli1 in Nup88-overexpressing cells appears to be dependent on the MEK-ERK pathway. (A) Expression of pERK1/2 in cells overexpressing GFP or Nup88-GFP was assessed by immunoblotting. (B) Statistical analysis of the expression of pERK1/2 shown in (A). Data represent mean ± SD (n=3). (C) Involvement of the MEK-ERK pathway in the expression of Gli1. GFP- or Nup88-GFP-overexpressing cells treated with or without the MEK1/2 inhibitor U0126 for 1 day were subjected to immunoblotting. Endogenous Nup88 is labeled as endo-Nup88. (D) Statistical analysis of the expression of Gli1 and pERK1/2 shown in (C). Data represent mean ± SD (n=3). (E) Expression of Gli1 and pERK1/2 in cells depleted of K-Ras. Expression of Gli1 and pERK1/2 was analyzed by immunoblotting in cells overexpressing GFP or Nup88-GFP with or without K-Ras depletion. α-Tubulin was used as a loading control. Endogenous Nup88 is labeled as endo-Nup88. (F) Statistical analysis of the expression of K-Ras, Gli1, and pERK1/2 shown in (E). Data represent mean ± SD (n=3). $^{*}P<0.05$, $^{**}P<0.01$, n.s., not significant. Gli1, glioma-associated oncogene homolog 1; Nup88, nucleoporin 88; p, phosphorylated; K-Ras, Kirsten's rat sarcoma virus.

increased in Nup88-GFP-overexpressing cells (Fig. 4A and B). Furthermore, blocking the phosphorylation of ERK with U0126, an inhibitor of MEK1/2, strongly suppressed the expression of Gli1 (Fig. 4C and D). These results indicated the involvement of the MEK-ERK pathway in Gli1 expression. Ras is a major upstream regulator of the MEK-ERK pathway;

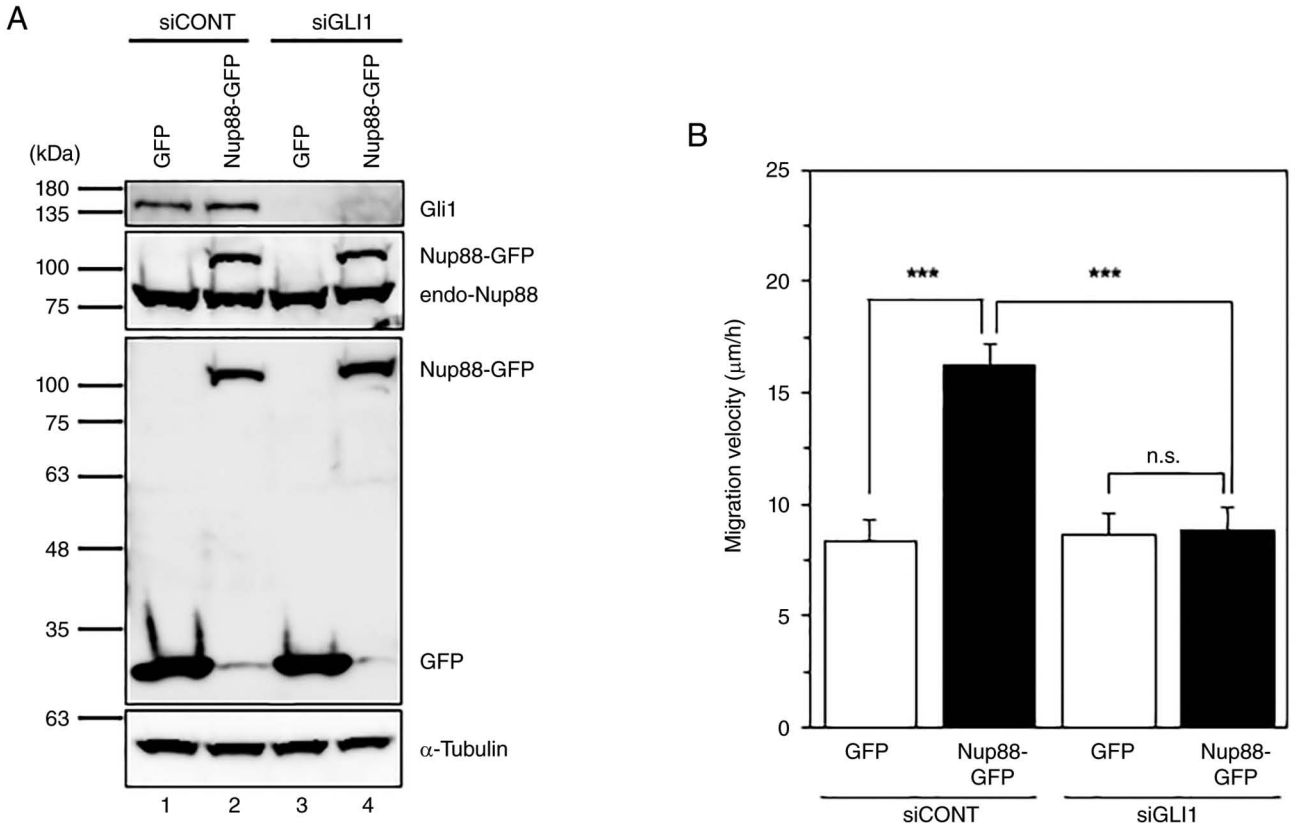

Figure 5. Enhanced migration of Nup88-overexpressing cells is Gli1-dependent. (A) Knockdown of *GLI1*. HeLa cells overexpressing GFP or Nup88-GFP were treated with control siRNA (siCONT) or *GLI1*-specific siRNA (siGLI1) for 2 days. Protein expression was analyzed by immunoblotting. Closed circle indicates a non-specific band detected by the anti-GFP antibody. α-Tubulin was used as a loading control. Endogenous Nup88 is labeled as endo-Nup88. Expression of Nup88-GFP was confirmed by immunoblotting using both anti-GFP and anti-Nup88 antibodies to verify the expression of the fusion protein. (B) Migration activity of Gli1-depleted cells overexpressing GFP or Nup88-GFP. Average migration velocity was calculated after tracking the cells for 24 h. In GFP-overexpressing cells, the average migration velocity of cells with control depletion or Gli1 depletion was 8.3 μm/h (n=73) and 8.6 μm/h (n=74), respectively. In Nup88-GFP-overexpressing cells, the average migration velocity of cells with control depletion or Gli1 depletion was 16.2 μm/h (n=75) and 8.8 μm/h (n=74), respectively. ***P<0.001, n.s., not significant. The data in (B) are based on the values obtained from Data S2. Nup88, nucleoporin 88; Gli1, glioma-associated oncogene homolog 1; si, small interfering; p, phosphorylated.

the present study therefore examined the involvement of Ras in the expression of Gli1. Among three Ras isoforms, Kirsten's rat sarcoma virus (K-Ras) is the predominant isoform in HeLa cells (37). When K-Ras was depleted by RNA interference, the level of pERK1/2 remained unchanged (Fig. 4E and F), suggesting that Nup88 activates the MEK-ERK pathway to regulate the expression of Gli1 independently of K-Ras.

Gli1 is involved in Nup88-dependent migration of HeLa cells. Aberrant expression of Gli1 induces various malignant phenotypes in cancer (23). Therefore, the present study examined whether increased expression of Gli1 in Nup88-overexpressing HeLa cells contributes to malignant phenotypes. To investigate the effect of Gli1 on motility, the migration velocity of Nup88-overexpressing HeLa cells with or without knockdown of Gli1 was monitored using live-cell single-cell imaging analysis. Knockdown of Gli1 in both cell lines was confirmed by immunoblotting (Fig. 5A). When control siRNA was transfected into both cell lines, the migration velocity of Nup88-GFP-overexpressing cells was nearly double that of GFP-overexpressing cells (Fig. 5B and Video S2). This finding was consistent with the result shown in Fig. 2C. By contrast, when *GLI1*-specific siRNA was transfected, the migration velocity of cells overexpressing Nup88-GFP was suppressed to a level comparable to that of cells overexpressing GFP (Fig. 5B and Video S2). These results indicate that the increase in Gli1 expression contributes to cell motility.

Nup88 regulates Kif7 and Gli1 through two independent pathways. The present study demonstrated that the overexpression of Nup88 in HeLa cells promoted cell migration through the epigenetic repression of Kif7 (Fig. 2) and the MEK-ERK pathway-dependent increase of Gli1 (Fig. 5). Since both Kif7 and Gli1 are components of the Hh signaling pathway, the possibility that the expression of these two proteins might be interdependently regulated was considered. Therefore, the present study examined the effect of Kif7 knockdown on the expression of Gli1, as well as the effect of the overexpression of Gli1 on the expression of Kif7. However, neither the knockdown of Kif7 (Fig. 6A-C) nor the overexpression of Gli1 (Fig. 6D and E) affected the expression of the other protein. These results suggested that the changes in expression of Kif7 and Gli1 are independent of each other.

Truncated Kif7 interacts with Gli1. The mechanism by which the truncated Kif7 suppresses the migration activity of Nup88-overexpressing cells remains unclear (Fig. 2). The present study considered two plausible mechanisms. One

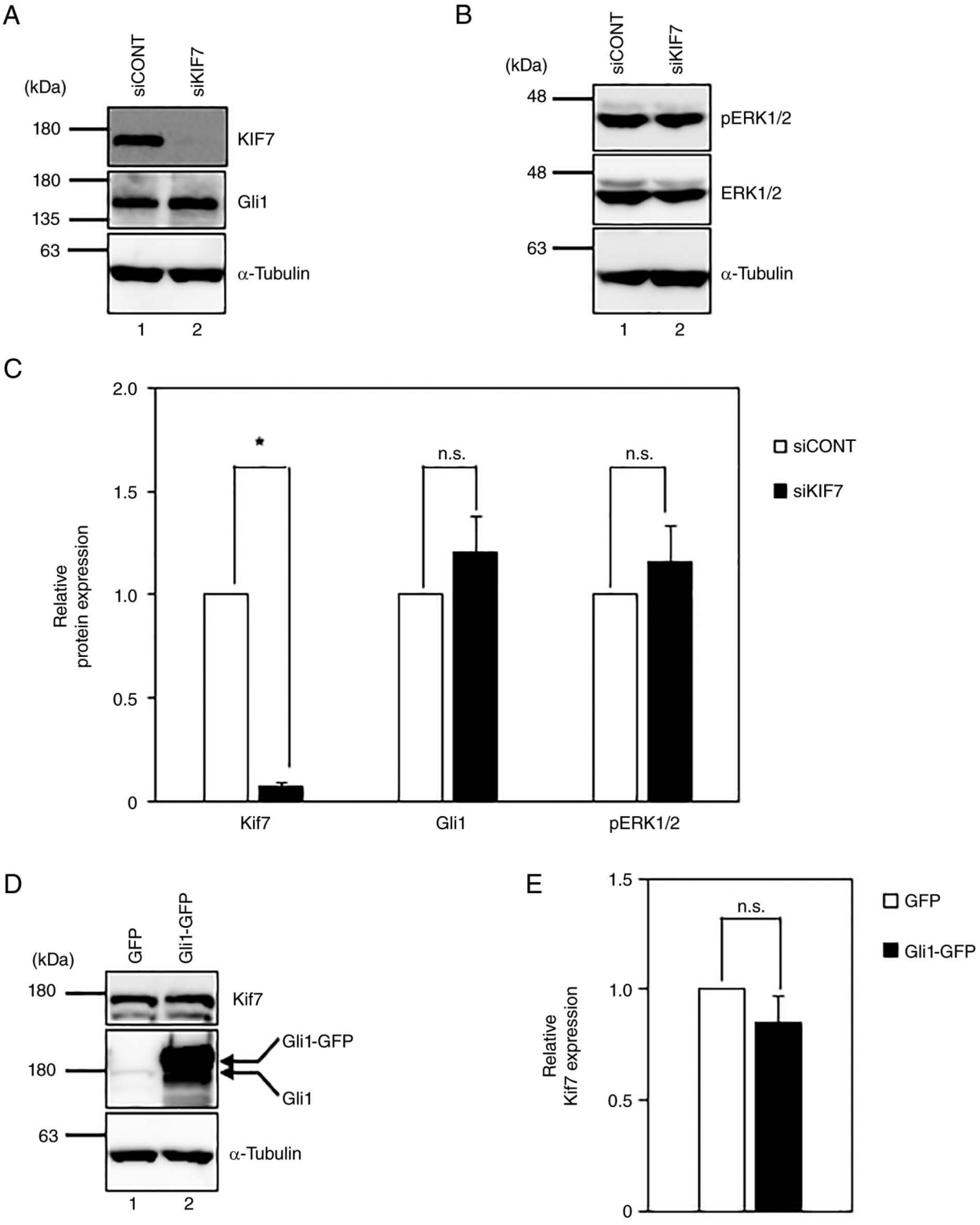

Figure 6. Mutual effects of the knockdown of Kif7 and the overexpression of Gli1 on their expression. Knockdown of Kif7. Control (siCONT) or *KIF7*-specific siRNA (siKIF7) was transfected into parental HeLa cells and the expression of Gli1 and pERK1/2 was analyzed by immunoblotting. The same cell lysates were loaded onto separate gels for the detection of (A) Gli1 and (B) pERK1/2. α-Tubulin was used as a loading control. (C) Statistical analysis of the expression of Kif7, Gli1, and pERK1/2 shown in (A and B). Data represent mean ± SD (n=3). (D) Overexpression of Gli1. HeLa cells overexpressing GFP or GFP-tagged Gli1 (Gli1-GFP) were analyzed by immunoblotting. α-Tubulin was used as a loading control. (E) Statistical analysis of the expression of Kif7 shown in (D). *P<0.05, n.s., not significant. Kif7, kinesin family member 7; si, small interfering; Gli1, glioma-associated oncogene homolog 1; p, phosphorylated.

possibility is that co-overexpression of the truncated Kif7 reduces the expression levels of phosphorylated ERK and/or Gli1. The other possibility is that the truncated Kif7 binds to Gli1 and suppresses its activity, as it does for Gli2/3, although the truncated Kif7 lacks a portion of the Gli2-binding domain. To address the former possibility, expression of phosphorylated ERK and Gli1 was examined in cells co-overexpressing Nup88-GFP and truncated Kif7. However, overexpression

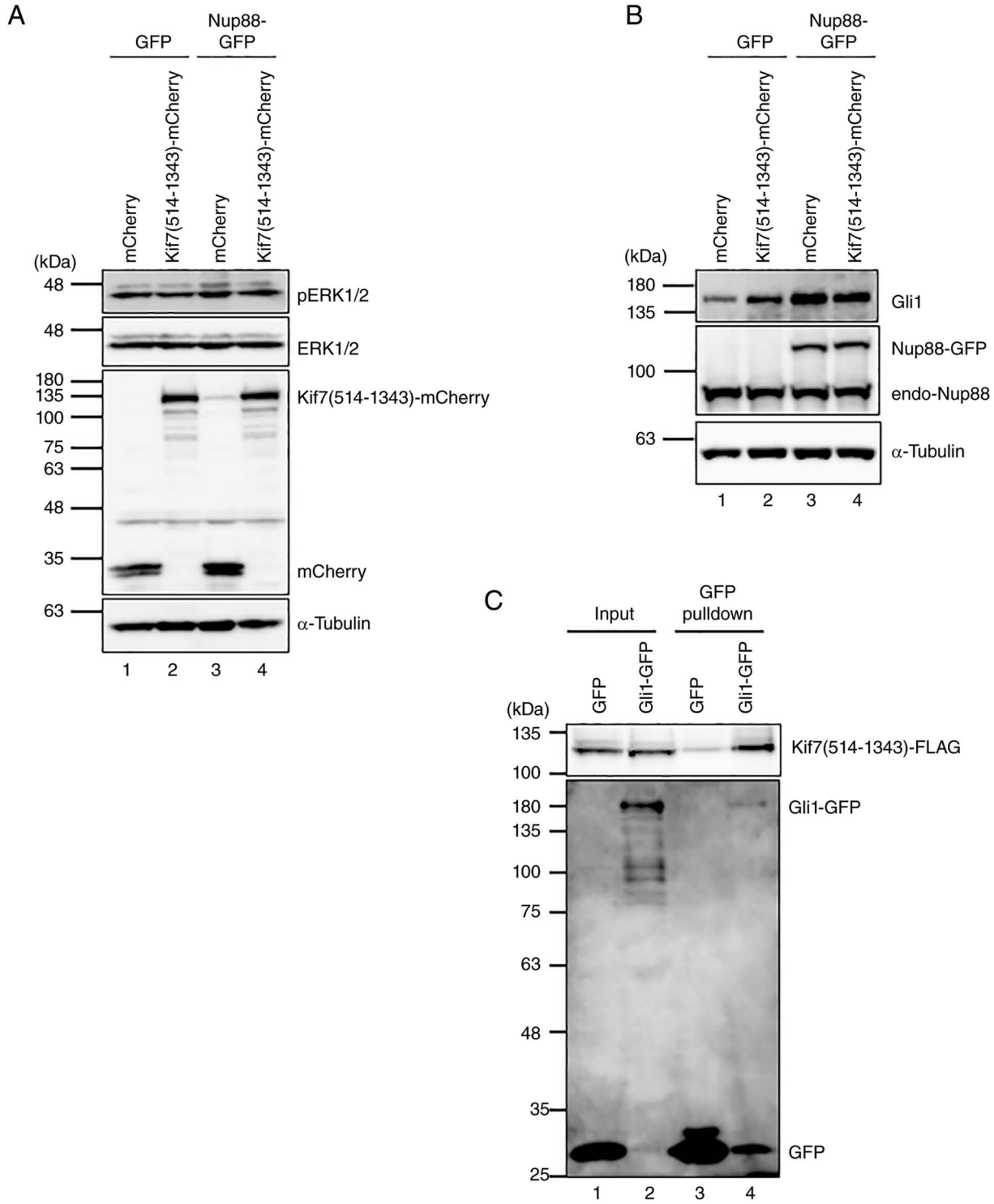

Figure 7. Truncated Kif7 interacts with Gli1. (A and B) Effect of truncated Kif7 on the expression of pERK1/2 and Gli1. mCherry or mCherry-tagged truncated Kif7 (Kif7(514-1343)-mCherry) was co-overexpressed in cells overexpressing GFP or Nup88-GFP, and the expression of pERK1/2 and Gli1 was analyzed by immunoblotting. The same cell lysates were loaded onto separate gels for the detection of (A) pERK1/2 and (B) Gli1. α-Tubulin was used as a loading control. Endogenous Nup88 is labeled as endo-Nup88. (C) GFP pulldown assay to analyze the interaction between Gli1 and the truncated Kif7. Cell lysates from parental HeLa cells co-overexpressing FLAG-tagged truncated Kif7 (Kif7(514-1343)-FLAG) together with either GFP or GFP-tagged Gli1 (Gli1-GFP) were subjected to a GFP pulldown assay. The resultant immunoprecipitated samples were then analyzed by immunoblotting. Kif7, kinesin family member 7; si, small interfering; Gli1, glioma-associated oncogene homolog 1; p, phosphorylated.

of the truncated Kif7 did not affect the expression of either phosphorylated ERK or Gli1 (Fig. 7A and B). For the latter possibility, a GFP-pulldown assay using parental HeLa cells co-overexpressing truncated Kif7 and GFP-tagged Gli1 was performed to test their interaction. The pulldown assay showed that the truncated Kif7 specifically co-precipitated with Gli1 (Fig. 7C). Taken together, these results suggested that the truncated Kif7 interacts with Gli1 and potentially sequesters it, thereby inhibiting its function without affecting its expression levels.

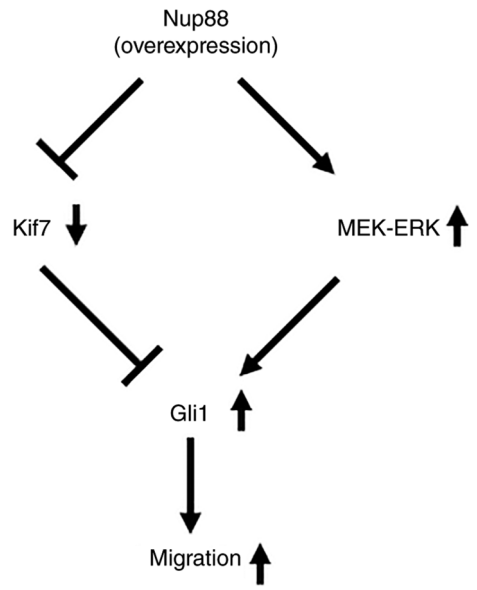

Figure 8. A mechanistic model for enhanced migration caused by Nup88. Stable overexpression of Nup88 in HeLa cells downregulates Kif7 and activates the MEK-ERK pathway, leading to increased expression and activation of Gli1, which in turn stimulates cell migration. Up arrow (↑) and down arrow (↓) indicate upregulation and downregulation, respectively. Nup88, nucleoporin 88; Kif7, kinesin family member 7; Gli1, glioma-associated oncogene homolog 1.

Discussion

The present study demonstrated that the migration of HeLa cells overexpressing Nup88 is enhanced by decreased expression of Kif7 and increased expression of Gli1. Moreover, the enhanced migration is suppressed by the knockdown of Gli1 or by the overexpression of the truncated Kif7 [Kif7(514-1343)], which interacts with Gli1. Based on these findings, the present study proposed a model to explain the mechanism by which overexpression of Nup88 promotes cell migration (Fig. 8). In the Nup88-overexpressing cells the present study established, Nup88 led to decreased expression of Kif7 and activation of the MEK-ERK pathway, which is required for the expression of Gli1. As knockdown of Kif7 did not activate ERK, Kif7 is unlikely to contribute to the increased expression of Gli1. Reciprocally, overexpression of Gli1 did not decrease the expression of Kif7. These findings suggested that the changes in expression of Kif7 and Gli1 occur independently of each other upon overexpression of Nup88. By contrast, migration induced by the overexpression of Nup88 was almost completely suppressed by either co-overexpression of the truncated Kif7 or knockdown of Gli1. Given that Kif7 binds to Gli1, this interaction may negatively regulate its function, as it does for Gli2 and Gli3. Thus, Kif7 likely suppresses migration through inhibiting the activity of Gli1, resulting in an effect similar to Gli1 knockdown.

In several prostate cancer cell lines, Kif7 expression appears to be, at least in part, epigenetically regulated. Indeed, it has been reported that the *KIF7* promoter region is hypermethylated in these cells and that treatment with DNA methylation inhibitors restores *KIF7* mRNA expression (29). However, the factor(s) that trigger epigenetic repression of *KIF7* remain unidentified. In the present study, HeLa cells stably overexpressing Nup88 exhibited decreased expression of Kif7, which was reversed by treatment with a DNA methylation inhibitor, as observed in prostate cancer cell lines. Therefore, Nup88 may function as an upstream factor that induces epigenetic repression of Kif7.

Increased expression of Gli1 in cancer cells can promote malignant phenotypes (23). In Nup88-overexpressing cells, expression of Gli1 appeared to be driven by the Ras-Raf-MEK-ERK pathway. However, knockdown of K-Ras did not affect expression of phosphorylated ERK, suggesting that there may be other upstream factors that activate the MEK-ERK pathway to stimulate expression of Gli1. NF-κB is one such candidate that can activate the MEK-ERK pathway (38). Specifically, overexpression of Nup88 in HeLa cells was reported to promote the nuclear accumulation of p65, an essential subunit of NF-κB involved in transcriptional activation (39). However, no nuclear accumulation of p65 was detected in the Nup88-overexpressing HeLa cells used in this study (32). Therefore, increased expression of Gli1 in these cells may be controlled by signaling molecules other than NF-κB, which connect with the MEK-ERK pathway.

Nup88-dependent migration was almost completely suppressed not only by the knockdown of Gli1 but also by the overexpression of the truncated Kif7 [Kif7(514-1343)]. Notably, this truncated Kif7 was still capable of binding to Gli1 despite lacking a portion of the coiled-coil domain (480-542 aa) responsible for binding to the zinc finger domain of Gli2, which is highly conserved among Gli proteins (40). Given that Kif7 is known to function as a negative regulator of Gli2/3, it is plausible that the interaction of the truncated Kif7 with Gli1 can inhibit Gli1 function. Indeed, Kif7 has additional predicted coiled-coil domains (698-1057 aa and 1109-1211 aa). Gli1 also possesses a zinc finger domain that is highly conserved among Gli proteins. Therefore, the truncated Kif7 may interact with Gli1 through one of these domains and thereby inhibit the function of Gli1. However, the possibility that Gli1 binds to the incomplete coiled-coil domain responsible for Gli2-binding cannot be ruled out.

In the present study, overexpression of Nup88 was shown to result in decreased expression of Kif7 and increased expression of Gli1, thereby enhancing cell migration. This observation may support the hypothesis that Nup88 is actively involved in the process of cancer progression. The clinical significance of the elevated expression of Nup88 has been reported in several types of cancers, where it primarily correlates with tumor grade and poor prognosis (18-20). For instance, in endometrial cancer, a positive correlation was observed between Nup88 mRNA levels and the depth of myometrial invasion (16). Similarly, in colorectal cancer, elevated expression of Nup88 was often observed at the invasive margin and in vascular-invaded areas of the primary and metastatic tumors (14). The finding of the present study that Nup88 modulates the expression levels of Kif7 and Gli1 in HeLa cells may provide a molecular basis for these clinical features. In cervical cancer, while early-stage tumors are generally responsive to conventional treatments such as surgery or radiochemotherapy, metastatic and recurrent cases present significant therapeutic challenges due to limited treatment options and poor prognosis. The findings of the present study suggested that sustaining Kif7 expression or inhibiting Gli1 could be an effective strategy to suppress Nup88-mediated migration. Given that Gli1 inhibitors are

already being investigated in clinical trials, this approach may also help overcome resistance to conventional therapies.

The findings of the present study offered key insights into Nup88-mediated migration in cervical cancer, yet its conservation in other cancers remains to be fully elucidated. Given that low expression of Kif7 correlates with poor prognosis in prostate, ovarian and breast cancers (41-43), investigating these malignancies will confirm the functional conservation of the Nup88 pathway and its viability as a therapeutic target.

Acknowledgments

The authors thank Dr Katharine Ullman (University of Utah, US) for providing HeLa cells.

Funding

The present study was supported by JSPS KAKENHI grant no. 19K07700.

Availability of data and materials

The data generated in the present study may be requested from the corresponding author.

Authors' contributions

MM, RU and AS designed and performed the experiments. MM and AK interpreted the results, wrote the manuscript and confirm the authenticity of all the raw data. All authors read and approved the final manuscript.

Ethics approval and consent to participate

Not applicable.

Patient consent for publication

Not applicable.

Competing interests

The authors declare that they have no competing interests.

References

1. Cronshaw JM, Krutchinsky AN, Zhang W, Chait BT and Matunis MJ: Proteomic analysis of the mammalian nuclear pore complex. J Cell Biol 158: 915-927, 2002.
2. Ribbeck K and Gorlich D: Kinetic analysis of translocation through nuclear pore complexes. EMBO J 20: 1320-1330, 2001.
3. Rout MP and Aitchison JD: The nuclear pore complex as a transport machine. J Biol Chem 276: 16593-16596, 2001.
4. Dickmanns A, Kehlenbach RH and Fahrenkrog B: Nuclear pore complexes and nucleocytoplasmic transport: From structure to function to disease. Int Rev Cell Mol Biol 320: 171-233, 2015.
5. Simon DN and Rout MP: Cancer and the nuclear pore complex. Adv Exp Med Biol 773: 285-307, 2014.
6. Snow CJ and Paschal BM: Roles of the nucleoporin Tpr in cancer and aging. Adv Exp Med Biol 773: 309-322, 2014.
7. Nofrini V, Di Giacomo D and Mecucci C: Nucleoporin genes in human diseases. Eur J Hum Genet 24: 1388-1395, 2016.
8. Hutten S and Kehlenbach RH: Nup214 is required for CRM1-dependent nuclear protein export in vivo. Mol Cell Biol 26: 6772-6785, 2006.
9. Bernad R, Engelsma D, Sanderson H, Pickersgill H and Fornerod M: Nup214-Nup88 nucleoporin subcomplex is required for CRM1-mediated 60 S preribosomal nuclear export. J Biol Chem 281: 19378-19386, 2006.
10. Bernad R, van der Velde H, Fornerod M and Pickersgill H: Nup358/RanBP2 attaches to the nuclear pore complex via association with Nup88 and Nup214/CAN and plays a supporting role in CRM1-mediated nuclear protein export. Mol Cell Biol 24: 2373-2384, 2004.
11. Xylourgidis N, Roth P, Sabri N, Tsarouhas V and Samakovlis C: The nucleoporin Nup214 sequesters CRM1 at the nuclear rim and modulates NFκB activation in Drosophila. J Cell Sci 119: 4409-4419, 2006.
12. Griffis ER, Xu S and Powers MA: Nup98 localizes to both nuclear and cytoplasmic sides of the nuclear pore and binds to two distinct nucleoporin subcomplexes. Mol Biol Cell 14: 600-610, 2003.
13. Agudo D, Gomez-Esquer F, Martinez-Arribas F, Nunez-Villar MJ, Pollan M and Schneider J: Nup88 mRNA overexpression is associated with high aggressiveness of Breast Cancer. Int J Cancer 109: 717-720, 2004.
14. Emterling A, Skoglund J, Arbman G, Schneider J, Evertsson S, Carstensen J, Zhang H and Sun XF: Clinicopathological significance of Nup88 expression in patients with colorectal cancer. Oncology 64: 361-369, 2003.
15. Knoess M, Kurz AK, Goreva O, Bektas N, Breuhahn K, Odenthal M, Schirmacher P, Dienes HP, Bock CT, Zentgraf H and Hausen AZ: Nucleoporin 88 expression in hepatitis B and C Virus-Related Liver Diseases. World J Gastroenterol 12: 5870-5874, 2006.
16. Schneider J, Martinez-Arribas F and Torrejon R: Nup88 expression is associated with myometrial invasion in endometrial carcinoma. Int J Gynecol Cancer 20: 804-808, 2010.
17. Zhao ZR, Zhang LJ, Wang YY, Li F, Wang MW and Sun XF: Increased serum level of Nup88 protein is associated with the development of colorectal cancer. Med Oncol 29: 1789-1795, 2012.
18. Martinez N, Alonso A, Moragues MD, Ponton J and Schneider J: The nuclear pore complex protein Nup88 is overexpressed in tumor cells. Cancer Res 59: 5408-5411, 1999.
19. Brustmann H and Hager M: Nucleoporin 88 expression in normal and neoplastic squamous epithelia of the uterine cervix. Ann Diagn Pathol 13: 303-307, 2009.
20. Gould VE, Martinez N, Orucevic A, Schneider J and Alonso A: A novel, nuclear pore-associated, widely distributed molecule overexpressed in oncogenesis and development. Am J Pathol 157: 1605-1613, 2000.
21. Xu S and Powers MA: Nuclear pore proteins and cancer. Semin Cell Dev Biol 20: 620-630, 2009.
22. Makise M, Uchimura R, Higashi K, Mashiki Y, Shiraishi R, Shutoku Y and Kuniyasu A: Overexpression of the nucleoporin Nup88 stimulates migration and invasion of HeLa cells. Histochem Cell Biol 156: 409-421, 2021.
23. Avery JT, Zhang R and Boohaker RJ: GLI1: A therapeutic target for cancer. Front Oncol 11: 673154, 2021.
24. Pietrobono S, Gagliardi S and Stecca B: Non-canonical hedgehog signaling pathway in cancer: Activation of GLI transcription factors beyond smoothened. Front Genet 10: 556, 2019.
25. Persson M, Stamataki D, Welscher P, Andersson E, Böse J, Rüther U, Ericson J and Briscoe J: Dorsal-ventral patterning of the spinal cord requires Gli3 transcriptional repressor activity. Genes Dev 16: 2865-2878, 2002.
26. Stone DM, Murone M, Luoh S, Ye W, Armanini MP, Gurney A, Phillips H, Brush J, Goddard A, de Sauvage FJ and Rosenthal A: Characterization of the human suppressor of fused, a negative regulator of the zinc-finger transcription factor Gli. J Cell Sci 112: 4437-4448, 1999.
27. Cheung HO, Zhang X, Ribeiro A, Mo R, Makino S, Puviindran V, Law KKL, Briscoe J and Hui CC: The kinesin protein Kif7 is a critical regulator of Gli transcription factors in mammalian hedgehog signaling. Sci Signal 2: ra29, 2009.
28. Niewiadomski P, Niedziolka SM, Markiewicz L, Uspienski T, Baran B and Chojnowska K: Gli Proteins: Regulation in development and cancer. Cells 8: 147, 2019.
29. Wong KY, Liu J and Chan KW: KIF7 attenuates prostate tumor growth through LKB1-mediated AKT inhibition. Oncotarget 8: 54558-54571, 2017.
30. Sung H, Ferlay J, Siegel RL, Laversanne M, Soerjomataram I, Jemal A and Bray F: Global cancer statistics 2020: GLOBOCAN Estimates of Incidence and Mortality Worldwide for 36 Cancers in 185 Countries. CA Cancer J Clin 71: 209-249, 2021.

31. Tewari KS: Cervical Cancer. N Engl J Med 392: 56-71, 2025.
32. Makise M, Nakamura H and Kuniyasu A: The role of vimentin in the tumor marker Nup88-dependent multinucleated phenotype. BMC Cancer 18: 519, 2018.
33. Kaiser C, Dobrikova EY, Bradrick SS, Shveygert M, Herbert JT and Gromeier M: Activation of cap-independent translation by variant eukaryotic initiation factor 4G in vivo. RNA 14: 2170-2182, 2008.
34. Livak KJ and Schmittgen TD: Analysis of relative gene expression data using real-time quantitative PCR and the $2^{-\widetilde{\Delta\Delta C}_T}$ method. Methods 25: 402-408, 2001.
35. Patel K, Dickson J, Din S, Macleod K, Jodrell D and Ramsahoye B: Targeting of 5-aza-2'-deoxycytidine residues by chromatin-associated DNMT1 induces proteasomal degradation of the free enzyme. Nucleic Acids Res 38: 4313-4324, 2010.
36. Capelson M, Liang Y, Schulte R, Mair W, Wagner U and Hetzer MW: Chromatin-bound nuclear pore components regulate gene expression in higher eukaryotes. Cell 140: 372-383, 2010.
37. Hood FE, Sahraoui YM, Jenkins RE and Prior IA: Ras protein abundance correlates with Ras isoform mutation patterns in cancer. Oncogene 42: 1224-1232, 2023.
38. Oeckinghaus A, Hayden MS and Ghosh S: Crosstalk in NF-κB signaling pathways. Nat Immunol 12: 695-708, 2011.
39. Takahashi N, van Kilsdonk JW, Ostendorf B, Smeets R, Bruggeman SWM, Alonso A, van de Loo F, Schneider M, van den Berg WB and Swart GWM: Tumor marker nucleoporin 88 kDa regulates nucleocytoplasmic transport of NF-κB. Biochem Biophys Res Commun 374: 424-430, 2008.
40. Haque F, Freniere C, Ye Q, Mani N, Wilson-Kubalek EM, Ku PI, Milligan RA and Subramanian R: Cytoskeletal regulation of a transcription factor by DNA mimicry via coiled-coil interactions. Nat Cell Biol 24: 1088-1098, 2022.
41. Ho J, Du Y, Wong OG, Siu MK, Chan KK and Cheung AN: Downregulation of the gli transcription factors regulator Kif7 facilitates cell survival and migration of choriocarcinoma cells. PLoS One 9: e108248, 2014.
42. Shagufta, Aftab M, Sisodiya S, Mishra S, Priya K and Hussain S: Prognostic significance of the kinesin superfamily in breast cancer: A systematic review & meta-analysis. Indian J Med Res 161: 627-635, 2025.
43. Yao Y, Liu L, He W, Lin X, Zhang X, Lin Z, Zeng Z and Guo S: Low expression of KIF7 indicates poor prognosis in epithelial ovarian cancer. Cancer Biomark 26: 481-489, 2019.